Published in final edited form as:
Cell Rep. 2013 May 30; 3(5): 1690–1702. doi:10.1016/j.celrep.2013.03.039.

A *Vibrio parahaemolyticus* T3SS Effector Mediates Pathogenesis by Independently Enabling Intestinal Colonization and Inhibiting TAK1 Activation

Xiaohui Zhou[1,2,3,4], **Benjamin E. Gewurz**[1,2,4], **Jennifer M. Ritchie**[1,2,3,5], **Kaoru Takasaki**[1], **Hannah Greenfeld**[1], **Elliott Kieff**[1,2], **Brigid M. Davis**[1,2,3], and **Matthew K. Waldor**[1,2,3,*]

[1]Division of Infectious Diseases, Brigham and Women's Hospital, 15 Francis Street, Boston, MA 02115, USA

[2]Department of Microbiology and Immunobiology, Harvard Medical School, 77 Ave Louis Pasteur, Boston, MA 02115, USA

[3]Howard Hughes Medical Institute, 181 Longwood Avenue, Boston, MA 02115, USA

SUMMARY

Vibrio parahaemolyticus type III secretion system 2 (T3SS2) is essential for the organism's virulence, but the effectors required for intestinal colonization and induction of diarrhea by this pathogen have not been identified. Here, we identify a type III secretion system (T3SS2)-secreted effector, VopZ, that is essential for *V. parahaemolyticus* pathogenicity. VopZ plays distinct, genetically separable roles in enabling intestinal colonization and diarrheagenesis. Truncation of VopZ prevents *V. parahaemolyticus* colonization, whereas deletion of VopZ amino acids 38–62 abrogates *V. parahaemolyticus*-induced diarrhea and intestinal pathology but does not impair colonization. VopZ inhibits activation of the kinase TAK1 and thereby prevents the activation of MAPK and NF-κB signaling pathways, which lie downstream. In contrast, the VopZ internal deletion mutant cannot counter the activation of pathways regulated by TAK1. Collectively, our findings suggest that VopZ's inhibition of TAK1 is critical for *V. parahaemolyticus* to induce diarrhea and intestinal pathology.

INTRODUCTION

Vibrio parahaemolyticus is a leading cause of diarrhea linked to the consumption of contaminated seafood worldwide (Su and Liu, 2007). Biopsies from patients infected with *V. parahaemolyticus* show disruption of the intestinal epithelium along with evidence of inflammation (Qadri et al., 2003), and similar signs of disease have been observed in ligated ileal loops in infected adult rabbits and in orally infected infant rabbits, both of which are used as animal models of *V. parahaemolyticus* infection (Park et al., 2004; Ritchie et al.,

*Correspondence: mwaldor@rics.bwh.harvard.edu.
[4]These authors contributed equally to this work
[5]Present address: Faculty of Health and Medical Sciences, University of Surrey, Guildford GU2 7XH, UK

SUPPLEMENTAL INFORMATION

Supplemental Information includes five figures and can be found with this article online at http://dx.doi.org/10.1016/j.celrep.2013.03.039.

2012). Analyses using these and other animal models strongly suggest that the virulence of this organism is dependent upon a type III secretion system (T3SS) encoded on *V. parahaemolyticus* chromosome II (T3SS2) (Park et al., 2004; Hiyoshi et al., 2010; Piñeyro et al., 2010; Ritchie et al., 2012). Strains lacking a functional T3SS2 fail to colonize the intestine of infant rabbits; they also do not induce signs of disease in ligated ileal loops, where factors that contribute solely to colonization are dispensable, suggesting that T3SS2 contributes to multiple facets of pathogenesis. An additional secretion system (T3SS1, encoded on chromosome I) has been linked to a variety of phenotypes in tissue culture-based assays, including cytotoxicity and cytokine induction (Park et al., 2004; Bhattacharjee et al., 2006; Burdette et al., 2008, 2009; Shimohata and Takahashi, 2010; Zhou et al., 2010; Broberg et al., 2011); however, T3SS1 appears to play only a minor role in pathogenesis within the gastrointestinal tract (Park et al., 2004; Ritchie et al., 2012). T3SS1 may instead contribute to *V. parahaemolyticus* interactions with some marine host(s) because this T3SS is found in all *V. parahaemolyticus* strains, including environmental/nonpathogenic isolates (Makino et al., 2003). In contrast, T3SS2 is largely absent from environmental/nonpathogenic isolates (Park et al., 2004).

T3SSs are essential for the virulence of several other Gram-negative pathogens, and they are used by bacteria to manipulate a variety of host cell processes that influence pathogen survival and growth (Coburn et al., 2007; Dean, 2011). These multicomponent molecular machines enable bacteria to transport proteins, referred to as “effectors,” from the bacterial cytoplasm, where they are synthesized, directly into the eukaryotic cell cytoplasm. Release of effectors from bacteria is typically triggered by contact between the pathogen and the host; however, secretion-inducing stimuli that are independent of host cells have also been identified. Effectors have been found to dampen the innate immune response, inhibit phagocytosis, reorganize cytoskeletal proteins to promote pathogen internalization, and modulate several other processes (Cornelis, 2006; Galán, 2009), and a single secretion system routinely transports multiple effectors with disparate functions. Some effectors have homologs that are translocated by secretion systems in a variety of organisms, whereas others are specific to a particular bacterial species or strain. In general, effectors show less cross-species conservation than do the structural components of the secretion apparati. Effectors are often, but not always, encoded adjacent to genes encoding the secretion machinery that enables their translocation.

To date, five effectors that are translocated by *V. parahaemolyticus* T3SS2 have been identified, all of which are encoded within or near the T3SS2 gene cluster. These proteins include a Ser/Thr acetyltransferase (VopA; Trosky et al., 2007), an actin nucleator (VopL; Liverman et al., 2007), an ADP ribosyltransferase (VopT; Kodama et al., 2007), an actin-bundling protein (VopV; Hiyoshi et al., 2011), and a homolog of cytotoxic-necrotizing factor, a deamidase (VopC; Akeda et al., 2011). However, with the exception of VopV, which has been shown to be critical for *V. parahaemolyticus*-induced enterotoxicity in rabbit ileal loops, there is no knowledge of the role of T3SS2 effectors in intestinal colonization or the pathogenesis of diarrhea, epithelial disruption, or inflammation caused by *V. parahaemolyticus*.

Here, we used two-dimensional (2D) gel electrophoresis to identify two proteins secreted by T3SS2, VPA1336 and VPA1350, as well as the likely needle component of T3SS2 (VPA1343). VPA1336, here renamed VopZ, proved to be a multifunctional effector that is essential for *V. parahaemolyticus* to colonize the intestine and to induce diarrhea. Notably, these two key virulence-related phenotypes appear to require different regions of VopZ. A *V. parahaemolyticus* mutant with a truncated *vopZ* did not colonize or cause diarrhea, whereas a mutant harboring a small internal deletion in *vopZ* robustly colonized but did not cause diarrhea or intestinal pathology. We demonstrate that VopZ inhibits activation of the

mitogen-activated protein kinase kinase kinase MAP3K7 (also called transforming growth factor β-activated kinase, or TAK1), a kinase important for the activation of both MAPK and NF-κB signaling pathways (Sakurai, 2012). In contrast, the VopZ internal deletion mutant cannot counter activation of pathways regulated by TAK1. Thus, VopZ's inhibition of TAK1 is dispensable for intestinal colonization by *V. parahaemolyticus*; however, it appears to be required for *V. parahaemolyticus* to cause intestinal pathology, including diarrhea and tissue disruption.

RESULTS

Previously Identified T3SS2 Effectors Do Not Play an Essential Role in Intestinal Colonization or Fluid Accumulation

Our group recently reported that infant rabbits are useful model hosts to investigate *V. parahaemolyticus* pathogenicity (Ritchie et al., 2012; Zhou et al., 2012b). Because we found that T3SS2 is critical for colonization, intestinal pathology, and diarrhea (Ritchie et al., 2012), we set out to identify and characterize T3SS2 effectors that could account for its pivotal role in pathogenesis. Our initial studies revealed that a *V. parahaemolyticus* mutant strain (derived from wild-type [WT] strain RIMD2210633; Makino et al., 2003) lacking the only three effectors confirmed at that time (VopT, VopA, and VopL) was fully pathogenic. The mutant and WT strains were equivalent in their ability to colonize rabbit intestines and induce diarrhea, intestinal fluid accumulation, and intestinal pathology (Figure S1; data not shown). The marked difference between the virulence of the *vopT vopL vopA* triple mutant and the *vscN2* mutant suggested that heretofore-unidentified T3SS2 effectors are essential for *V. parahaemolyticus* intestinal colonization and disease.

Identification of T3SS2-Secreted Proteins

To identify T3SS2-secreted effectors, we used 2D difference gel electrophoresis (DIGE) to compare proteins secreted by a T3SS1-deficient strain (RIMD2210633 *vscN1*; Hiyoshi et al., 2010) and a T3SS1/T3SS2-deficient strain (RIMD2210633 *vscN1 vscN2*; Hiyoshi et al., 2010). This approach enabled detection of 30 potential T3SS2-dependent-secreted proteins, 23 of which were found to be encoded by *V. parahaemolyticus*, and 19 of which were encoded in the genomic island that yields T3SS2 (Figure 1). The T3SS2-encoded polypeptides (derived from 11 annotated proteins) included VopL, VopT, VopA, two effectors reported to be secreted via T3SS2 after this study was initiated (VopV and VopC) (Akeda et al., 2011; Hiyoshi et al., 2011), VopD2 and VopW (components of the T3SS2 translocon, a portion of the secretion apparatus that is itself often secreted) (Kodama et al., 2008; Zhou et al., 2012b), and VopcC, which is thought to function as the chaperone for VopC (Akeda et al., 2011). Additionally, the uncharacterized T3SS2-encoded proteins VPA1336 (named here VopZ), VPA1350, and VPA1343 appeared to be secreted in a T3SS2-dependent fashion. Secretion of VPA1336 and VPA1350 was also suggested by recent observations using a heterologous expression system (Zhou et al., 2012a).

VPA1350 and VPA1343 Are Required for T3SS2- Dependent Protein Secretion and/or Translocation—As an initial step in determining the significance of previously uncharacterized potential effectors, we examined whether strains harboring mutations in *vpa1343*, *vopZ*, or *vpa1350* were impaired for secretion or translocation of known T3SS2 substrates. Neither deletion of *vpa1350* nor introduction of a stop codon into amino acid (aa) 41 of the VPA1336 ORF (subsequently termed *vopZ*′) reduced release of VopD2 into culture supernatants; however, supernatant from a *vpa1343* deletion mutant did not contain detectable VopD2, despite the presence of this protein in cell pellets (Figure S2A). These results suggest that VPA1343 is either a component of the T3SS2 secretion apparatus or that the *vpa1343* deletion had polar effects. Consistent with the former possibility, bioinformatic

analysis (http://www.sbg.bio.ic.ac.uk/phyre2/html/page.cgi?id=index; Kelley and Sternberg, 2009) suggests that VPA1343 is a structural homolog of PrgI, the needle protein for the *Salmonella enteriditis* SPI-1 T3SS. Subsequent immunofluorescence microscopy-based analyses of effector translocation by the *vopZ*′ and *vpa1350* mutants revealed that *vpa1350* (but not *vopZ*) is required for this process; translocation of VopV was equivalent from a *vscN1* mutant (the positive control strain) and from a *vscN1 vopZ*′ mutant, whereas no VopV translocation was apparent from the *vpa1350* deletion mutant (Figure S2). Thus, it seems likely that VPA1350, like VPA1343, plays a structural or regulatory role in the translocation process. The relative abundance of VPA1350 seen with DIGE is also consistent with its being a component of the secretion apparatus; structural proteins were in general significantly more abundant than were effectors (Figure 1).

VopZ Is Translocated into Eukaryotic Cells in a T3SS2-Dependent Manner

Western blot analyses (data not shown) confirmed the initial DIGE-based observation that VopZ (and also VPA1350) is secreted into culture supernatants in a T3SS2-dependent manner. Furthermore, by comparing cAMP activity in Caco-2 cells infected with *vscN1* or *vscN1 vscN2 V. parahaemolyticus* strains that produce various effector-Cya (adenylate cyclase) fusion proteins, we found that VopZ-Cya is translocated as efficiently as the known effector VopV (Figure S2C). Thus, in contrast to VPA1350 and VPA1343, VopZ appears to be a secreted and translocated protein that, like most T3SS effectors, is not required for secretion or translocation of other T3SS2 substrates.

VopZ Forms Punctae in HeLa Cells

N-terminally HA-tagged VopZ formed discrete cytoplasmic punctae in transfected HeLa cells (Figure S3). Transfection of a series of truncated *vopZ* derivatives suggested that aa 38–62 of VopZ are important for puncta formation (Figure S3); in the absence of these aa (e.g., VopZ63–251 and VopZΔ38–62), VopZ was distributed diffusely in the HeLa cell cytoplasm. Notably, this region of VopZ is highly conserved among VopZ homologs (which are all hypothetical, uncharacterized proteins), suggesting that it may be important for VopZ function. BLAST and Phyre analyses of VopZ did not reveal the presence of known conserved domains or significant similarities with known protein structures.

VopZ Is Required for the T3SS2-Dependent Inhibition of IL-8 Secretion

In previous studies, T3SS2 was reported to limit production of transcripts for IL-8, a proinflammatory CXC chemokine (Matlawska-Wasowska et al., 2010); however, no T3SS2 effector was linked to this phenotype. Therefore, we explored whether VopZ modulates production of IL-8 by infected HEK293 and HeLa cells. Experiments were performed with bacteria lacking *vscN1*, an integral component of T3SS1, because this system induces host cell cytotoxicity and lysis that complicates other analyses. As previously reported, we found that T3SS2 suppresses IL-8 production in response to *V. parahaemolyticus* infection: a *vscN1 vscN2* strain, in which both T3SS1 and T3SS2 are inactive, induced markedly more IL-8 secretion by HEK293 cells than did a *vscN1* strain. Notably, this suppression appears to be entirely dependent upon VopZ because the *vscN1 vopZ*′ and *vscN1 vscN2* mutants similarly induced IL-8 production (Figure 2A). VopZ also blocks IL-8 upregulation by HEK293 cells in response to TNF-α, a potent stimulator of IL-8 production that is induced during infection of infant rabbits with *V. parahaemolyticus* (Ritchie et al., 2012). TNF-α-stimulated HEK293 cells cocultured with either the *vscN1 vopZ*′ or the *vscN1 vscN2* mutants produced significantly more IL-8 than cells cocultured with the *vscN1* strain that translocates VopZ (Figure 2A). Furthermore, reintroduction of WT *vopZ* into the *vscN1 vopZ*′ mutant reduced IL-8 levels, both in the absence and presence of TNF-α, confirming that disruption of *vopZ* accounts for the phenotype of the *vopZ*′ mutant. VopZ also blocked IL-8 upregulation in HeLa cells in response to IL-1β (Figure 2B), suggesting that VopZ acts

upon a shared component of the IL-1β and TNF-α response pathways, rather than a receptor-specific element. Finally, VopZ aa 38–62, which were important for punctae formation, also appeared to be important for inhibition of IL-8 production. Cells infected with *vscN1 vopZΔ38–62* and *vscN1 vopZ′* secreted indistinguishable amounts of IL-8, in response to both TNF-α and IL-1β (Figures 2A and 2B). Notably, the *vopZΔ38–62* mutation did not impair VopZ translocation (Figure S2C), nor did it affect adhesion of *V. parahaemolyticus* to host cells (data not shown), suggesting that aa 38–62 contribute directly to the protein's effect on the host cell signaling pathways involved in IL-8 production.

VopZ Inhibits NF-κB Activation

Induction of IL-8 production in response to TNF-α, IL-1β, and/or bacterial infection is largely dependent on NF-κB and MAPK pathway activation (Hoffmann et al., 2002). To begin to define how VopZ inhibits IL-8 production, we tested whether VopZ altered TNF-α-induced translocation of the p65 (RelA) subunit of NF-κB into the nucleus, which is necessary for canonical NF-κB pathway target gene induction. HeLa cells were infected with *V. parahaemolyticus* for 1 hr (which is sufficient for T3SS2 effector translocation) and then stimulated with TNF-α. Subsequent analysis of p65 subcellular localization, using confocal immunofluorescence microscopy, revealed that nuclear p65 was far less evident in cells infected with *vscN1 V. parahaemolyticus* (20% of cells) than in uninfected cells (78% of cells; Figure 2Ca versus Figure S4). In comparison to *vscN1*-infected cells, nuclear p65 was twice as prevalent in *vscN1 vscN2*, *vscN1 vopZ′*, and *vscN1 vopZΔ38–63*-infected cells (53%, 44%, and 40%, respectively, of cells; Figure 2C). There is no statistically significant difference between p65 translocation by cells infected with the three strains of *V. parahaemolyticus* that lack intact *vopZ* or *vscN2*; however, infection by all three mutants appears to have a residual effect on p65 translocation (relative to uninfected cells; $p < 0.05$), suggesting that *V. parahaemolyticus* also has T3SS1- and T3SS2-independent means of modulating this process. The phenotype of the *vopZ′* mutant could be complemented by plasmid-expressed VopZ (Figure 2Ce; 22.6% nuclear p65). Transfected VopZ similarly inhibited p65 nuclear translocation in HeLa cells. Thirty minutes following TNF-α treatment, only 19% of VopZ-transfected cells contained nuclear p65, versus 78% of untransfected cells (Figure S4). By contrast, transfected VopZΔ38–62 had minimal effect on p65 translocation (Figure S4). These analyses suggest that VopZ inhibits IL-8 production, at least in part, by preventing p65 nuclear translocation.

A variety of additional experiments confirmed that VopZ inhibited NF-κB activation. To confirm that VopZ blocks NF-κB target gene upregulation, we used HEK293 cells containing a stably integrated GFP reporter of NF-κB pathway activity (Gewurz et al., 2011). TNF-α stimulation similarly upregulated GFP expression in uninfected cells and in cells infected with the *vscN1 vscN2*, *vscN1 vopZ′*, or *vscN1 vopZΔ38–62* strains for 90 min prior to TNF-α treatment. In contrast, cells infected with the *vscN1* strain exhibited significantly lower NF-κB GFP reporter intensity in response to TNF-α treatment (Figures 3A and 3B). VopZ also modulated NF-κB reporter activation in response to *V. parahaemolyticus* in the absence of TNF-α stimulation (Figure 3C), as seen above for IL-8 production.

To further characterize the mechanism of VopZ function, we studied its effect on turnover of IκBα, an inhibitory factor that retains p65 NF-κB complexes in the cytosol (Hayden and Ghosh, 2012). Canonical NF-κB pathways trigger activation of the kinase IKK-β, which phosphorylates IκBα and triggers its proteasomal degradation (Hayden and Ghosh, 2012). In HEK293 cells infected with *V. parahaemolyticus* and subsequently treated with TNF-α, the presence of VopZ (but not VopZΔ38–62) prevented IκBα degradation that was otherwise apparent within 15 min of TNF-α treatment (Figures 3D and 3E). Collectively,

these results indicate that VopZ blocks canonical NF-κB activation at or above the level of IκBα degradation and that this effect requires VopZ residues 38–62.

V. parahaemolyticus Infection Does Not Inhibit Noncanonical NF-κB Pathway Activation

Signaling via the noncanonical NF-κB pathway triggers activation of the IKK-α kinase, which phosphorylates p100, the precursor of the p52 NF-κB transcription factor. This phosphorylation triggers p100 cleavage into the active p52 form, followed by nuclear translocation of p52 homodimers and p52/RelB heterodimers (Sun, 2011). We tested whether VopZ can block noncanonical NF-κB activation using HEK293 cells that inducibly express the Epstein-Barr virus Latent Membrane Protein 1 (LMP1), a potent activator of this pathway (Luftig et al., 2004). In contrast to its inhibitory effects on the canonical pathway, *V. parahaemolyticus* infection did not block generation of p52 in response to LMP1 expression (Figure 3F). These data suggest that VopZ's target is a component of the canonical, but not the noncanonical, pathway for NF-κB activation.

VopZ Inhibits MAPK Pathway Activation

Many of the stimuli that lead to NF-κB activation (e.g., cytokines and various ligands for Toll-like receptors) concurrently activate both canonical NF-κB and pathways regulated by the MAPKs JNK and p38. Therefore, we explored whether VopZ also impairs activation of these MAPKs, which could indicate that it targets a factor common to these pathways. JNK and p38 kinase activation loop phosphorylation was used as a readout of their activation state. We observed, using HEK293 cells infected with *V. parahaemolyticus* and subsequently stimulated with TNF-α, that JNK and p38 phosphorylation (but not protein abundance) was markedly lower following infection with the *vscN1* or *vscN1 vopZ′* pVopZ strains than with the *vscN1 vscN2*, *vscN1 vopZ′*, or *vscN1 vopZΔ38–62* strains (Figures 4A and 4B). Furthermore, infection with *V. parahaemolyticus* strains that lack VopZ triggered MAPK phosphorylation even prior to TNF-α stimulation, which was also blocked by VopZ. These results suggest that VopZ antagonizes multiple MAPK pathways and that as for NF-κB, this inhibitory effect is dependent upon VopZ aa 38–62.

VopZ Prevents TAK1 Activation

The cellular pathways leading to canonical NF-κB activation and MAPK induction in response to several ligands, including IL-1β and TNF-α, converge at TAK1 (Sakurai, 2012; Hayden and Ghosh, 2011), which is not a component of the noncanonical NF-κB activation pathway (Figure 5A). Thus, altered activation of TAK1 could account for all the effects of VopZ that we have observed. In support of this hypothesis, we observed that the presence of VopZ prevented accumulation of TAK1 phosphorylated on Thr184 in HEK293 cells infected with *V. parahaemolyticus*, both in response to the bacteria alone (Figure 5B, time = 0 min) and in response to bacterial infection followed by TNF-α treatment (Figure 5B, time = 15 min). Such activation loop phosphorylation is important for the induction of TAK1 activity (Kishimoto et al., 2000). Furthermore, full-length VopZ prevented the autophosphorylation of TAK1 that occurs upon its overexpression in transfected HEK293 cells, as well as subsequent activation of its downstream target p38 (Figure 5C). In contrast, VopZ had no effect upon phosphorylation/autoactivation of transfected MKK6 or on MKK6-mediated phosphorylation of p38 (Figure 5D). Finally, infection with the *vscN1* mutant, but not the *vscN1 vopZ′* strain, impaired the kinase activity of transfected TAK1. Following 90 min of coculture with *V. parahaemolyticus*, FLAG-tagged TAK1 was immune purified from transfected HEK293 cells and tested in an in vitro kinase assay with recombinant kinase-deficient MKK6 ($MKK6^{K82A}$) (Paquette et al., 2012). TAK1 purified from cells infected with the *vscN1 vopZ′* strain was significantly more active than that purified from cells cocultured with the *vscN1* mutant, even though there were very similar amounts of TAK1 in the assays (Figure 5E). Collectively, these data strongly suggest that

VopZ inhibits activation of MAPK and the canonical NF-κB pathway via limiting accumulation of activated TAK1 (Figure 5A).

VopZ Contributes to *V. parahaemolyticus* Intestinal Colonization and Disease in Infant Rabbits

We used the infant rabbit model of *V. parahaemolyticus* infection to explore whether this pathogen requires VopZ to colonize the small intestine and/or cause disease. Strikingly, truncation of VopZ (i.e., *vopZ′*) reduced intestinal colonization, diarrhea/fluid accumulation, and intestinal pathology to nearly the same extent as did inactivation of the entire T3SS2 (via deletion of *vscN2*) (Figure 6), even though our vitro analyses suggest that T3SS2 is fully functional in a *vopZ′* background. The effect of *vopZ* truncation on colonization and fluid accumulation was eliminated when the mutant strain contained a plasmid encoding WT VopZ, thereby confirming that the *vopZ′* mutation accounts for the mutant's phenotypes (Figures 6A and 6B). These data indicate that VopZ, unlike all T3SS2 effectors described to date, is critical for *V. parahaemolyticus* colonization and disease.

Interestingly, in contrast to all assays described above, the effects in infant rabbits of the *vopZ′* and *vopZΔ38–62* mutations were not equal. The absence of VopZ aa 38–62, unlike VopZ truncation, did not interfere with the capacity of *V. parahaemolyticus* to colonize the infant rabbit intestinal tract (Figure 6A). Thus, VopZ's contribution to intestinal colonization does not appear to be dependent on modulation of TAK1 activation, suggesting that VopZ must have an additional, and genetically separable, function. Notably, deletion of VopZ aa 38–62 also did not influence infiltration of heterophils into intestinal tissue (Figure S5A), and the presence of WT VopZ versus VopZΔ38–62 did not affect the abundance of transcripts for IL-8, TNF-α, and IL-1β in intestinal tissue (data not shown). However, it should be noted that in vivo, these markers of inflammation can be induced by numerous stimuli and pathways and are not expected to be fully dependent upon epithelial cell TAK1.

Furthermore, although this internal *vopZ* deletion did not reduce the bacterial load or appear to influence several markers of inflammation in the rabbit intestine, this mutation nonetheless had a dramatic effect upon critical signs of disease. The *vopZΔ38–62* mutation eliminated gross manifestations of infection, including diarrhea and fluid accumulation, in infected rabbits (Figure 6B). As seen in vitro, the absence of VopZ aa 38–62 was also associated with an increase in the frequency of nuclear p65, consistent with the role of these aa in blocking TAK1 activation (Figure 7A). Additionally, the *vopZΔ*38–62 mutation markedly reduced the epithelial disruption typically observed with *V. parahaemolyticus* infection (Figure 7B). The presence of WT VopZ, rather than VopZΔ38–62, was associated with increased epithelial cell sloughing (Figure 6C) and disruption of filamentous actin at the villus surface (Figure S5B), alterations likely to reflect a loss of epithelial barrier function. These observations are consistent with previous analyses that have reported disruption of the murine intestinal epithelium and loss of barrier function in response to TAK1 deficiency (Kajino-Sakamoto et al., 2008, 2010). Coupled with our in vitro data, our in vivo results suggest that VopZ-dependent inhibition of TAK1 activation is critical to the development of *V. parahaemolyticus*-linked intestinal pathology.

DISCUSSION

Previous studies using animal models of *V. parahaemolyticus* pathogenicity have revealed that T3SS2 is critical for this pathogen to colonize the intestine and to cause disease (Park et al., 2004; Hiyoshi et al., 2010; Piñeyro et al., 2010; Ritchie et al., 2012). Here, we found that VopA, VopT, and VopL—the three T3SS2-secreted effectors known when this work was initiated—are not required by *V. parahaemolyticus* to colonize the infant rabbit intestine or induce disease. Additionally, we identified T3SS2-secreted proteins, two of which

(VPA1343 and VPA1350) are likely to be components of the secretion/translocation apparatus. The third protein, VopZ (VPA1336), is an uncharacterized T3SS2-encoded/-secreted polypeptide with no recognizable functional domains. We discovered that VopZ, unlike VopA, VopT, and VopL, is an essential virulence factor. Furthermore, VopZ appears to play distinct, genetically separable roles in enabling *V. parahaemolyticus* to colonize the intestine and to cause diarrhea. Truncation of VopZ prevented *V. parahaemolyticus* colonization as well as all signs of disease; however, deletion of VopZ aa 38–62 abrogated *V. parahaemolyticus*-induced diarrhea/intestinal fluid accumulation and most histopathologic signs of disease but did not impair *V. parahaemolyticus*' capacity to colonize the small intestine, indicating that regions outside of VopZ aa 38–62 mediate VopZ's role in colonization. The correlation between VopZ aa 38–62 dependent inhibition of TAK1 in vitro, aa 38–62 dependent diarrhea and other intestinal pathology in vivo, and the previously described consequences of intestinal TAK1 deficiency strongly suggests that inhibition of TAK1 activation by VopZ is a critical facet of *V. parahaemolyticus* pathogenicity.

VopZ differs from the vast majority of T3SS-secreted effectors in that it is essential for the virulence of the organism that produces it. Intestinal colonization by *V. parahaemolyticus* lacking VopZ is reduced by several orders of magnitude relative to the WT strain, and infected animals do not display overt signs of infection, such as diarrhea or intestinal fluid accumulation. In contrast, deletions of individual T3SS effectors in other organisms, like our deletions of the previously described T3SS2 effectors VopA, VopT, and VopL, frequently have a relatively subtle effect on pathogenesis (Galán, 2009; Dean, 2011). One of the few effectors known to be required for virulence is the EHEC protein Tir, which enables formation of the hallmark tight association between the bacteria and the host tissue. However, our in vitro analyses (data not shown) suggest that mutations in *vopZ*, unlike those in *tir* (DeVinney et al., 1999), do not impair adherence of bacteria to eukaryotic cells. Future analyses will aim to identify the precise regions of VopZ, as well as the mechanisms, that enable VopZ to contribute to intestinal colonization.

TAK1, whose activation we found was effectively blocked by VopZ (Figure 5), has previously been shown to have a profound effect on maintenance of intestinal integrity. The absence of TAK1 in the intestinal epithelium results in a plethora of phenotypes, including inflammation, apoptosis of crypt cells, distorted epithelial structure, mislocalization of tight junction proteins, and reduced transepithelial resistance (Kajino-Sakamoto et al., 2008). TAK1-deficient intestinal epithelium also contains increased levels of reactive oxygen species and is hypersensitive to oxidative stress (Kajino-Sakamoto et al., 2010). Thus, even though TAK1 activation has consequences associated with inflammation (e.g., NF-κB and MAPK signaling) in an in vitro system, in the more complex milieu of an intact organism, TAK1 deficiency is also associated with inflammation. Similarly, conditional ablation of IKK-γ, a scaffold necessary for canonical NF-κB activation, produced enterocyte damage, which then allows bacterial translocation and dramatic Toll-like receptor-dependent inflammation in vivo (Nenci et al., 2007). Thus, whereas in vitro analyses using a homogeneous cell population are extremely valuable for precise dissection of signal transduction pathways and their regulatory processes, they often fail to fully represent the complex phenotypes that can ensue from the interplay of multiple cell types and flora within the intact intestine. It is likely that the differences we have observed between the role of VopZ in vitro and in vivo (e.g., VopZ's lack of an effect in vivo on total cytokine levels) are analogous to those seen in analyses of TAK1 in vitro and in vivo, in that they are a consequence of the greater complexity of the in vivo system.

In contrast to the engineered mice, where TAK1 is uniformly deficient in the intestinal epithelium, mice infected with *V. parahaemolyticus* likely have suppressed TAK1 activity

only in a subset of cells. During infection, *V. parahaemolyticus* generally forms discrete clusters rather than being distributed across the epithelial surface (Ritchie et al., 2012), and VopZ and other T3SS2 effectors are thus unlikely to be transmitted to the entire intestinal epithelium. Consequently, VopZ's effects on TAK1 signaling are probably best measured at the level of single cells, such as the changes we observed in p65 nuclear translocation or in the actin cytoskeleton, rather than tissue wide, such as changes in gene expression or in the level of secreted factors. Still, there are noteworthy similarities between the reduced epithelial integrity observed in response to TAK1 deficiency and infection with VopZ-secreting *V. parahaemolyticus*. Further- more, local disruptions in tissue integrity (e.g., in response to translocated VopZ) can have a profound effect upon its barrier function, for example by allowing bacterial translocation that can subsequently provoke a vigorous immune response and/or serve as a trigger for more comprehensive disruption (Baldwin, 2012). Such local disruptions are thought to underlie the role in virulence of YopJ (discussed below), a T3SS effector in *Yersinia* with somewhat analogous effects on signaling to those of VopZ. Our analyses of VopZ's significance in vitro and in vivo suggest that focal inhibition of TAK1 activity in the intestinal epithelium has a marked effect upon the integrity of this tissue and plays a critical role in the virulence of *V. parahaemolyticus*.

Numerous factors and pathways are known to lead to TAK1 activation, including TNF-α and other cytokines, LPS, DNA damage, osmotic shock, and hypoxia (Dai et al., 2012). It has also been proposed that different processes govern basal versus stimulus-dependent TAK1 activation, mediated by the TAK1-associated proteins TAB1 and TAB2/TAB3, respectively (Omori et al., 2012). The fact that VopZ inhibits TAK1's activation via a variety of agents and activating processes (e.g., IL-1β, TNF-α, and microbe-dependent activation) whose pathways converge at the level of TAK1 activation, suggests that it likely acts either on TAK1 itself or on a factor that is routinely associated with it, such as TAB1. Our finding that VopZ inhibits TAK1 activation following transfection and overexpression —a process that is thought to be mediated by enhanced TAK1 oligomerization and to be independent of upstream stimuli—also supports that idea that VopZ acts at the level of the TAK1 protein complex, rather than in upstream activation pathways. VopZ might interfere with induction of the TAK1 conformational shift that is thought to enable activating autophosphorylation, either via interacting with a TAB protein or with TAK1 itself. Alternatively, VopZ might increase the activity of a TAK1-associated phosphatase, such as the type 2A protein phosphatase PP6 (Kajino et al., 2006), or possess phosphatase activity itself, although no conserved enzymatic domains were detected. The TAK1-inhibitory activity of VopZ was correlated with punctate localization of VopZ; however, it is currently unclear whether VopZ's localization directly contributes to its activity.

Although VopZ is not homologous to known T3SS effectors, other effectors are known to interfere with TAK1 activity. The best characterized of these is the *Yersinia* protein YopJ, an acetyltransferase. YopJ acetylates the activation loop of TAK1, which inhibits TAK1 phosphorylation/activation, and thereby prevents activation of downstream pathways (Meinzer et al., 2012; Paquette et al., 2012). YopJ, like VopZ, contributes to disruption of the intestinal epithelium and its barrier function during infection (Meinzer et al., 2012). However, it should be noted that YopJ has multiple additional substrates, including MKK6, p38, JNK, and IKKβ (Mittal et al., 2006; Mukherjee et al., 2006); consequently, the pathways modulated by YopJ and VopZ may not entirely coincide. The EPEC/EHEC protein NleE also reduces TAK1 activation by methylating TAB2 and TAB3 (Zhang et al., 2012), but roles for this effector during infection have yet to be described. Additional effectors, such as VopA, AvrA, OspF, SpvC, and HopAI1, have been found to target factors downstream of TAK1, such as MAPKKs and MAPKs, suggesting that disruption of the pathways controlled by TAK1 is beneficial for a variety of pathogens (Galán, 2009; Dean, 2011). In our experiments, it is somewhat surprising that we do not observe more inhibition

of the MAPK pathways by the *vopZ* mutants versus the *vscN2* mutant because the former strains still produce VopA; this result suggests that VopZ may be the dominant inhibitor of MAPKs generated by *V. parahaemolyticus*.

Finally, our findings may have potential clinical applications. First, because the *V. parahaemolyticus vopZΔ38–62* mutant robustly colonizes the intestine yet does not cause diarrhea, it may be possible to create a live attenuated *V. parahaemolyticus* vaccine based on this strain. Optimization of *vopZΔ38–62*-based vaccine may require inclusion of additional attenuating mutations. Such a vaccine could also potentially deliver heterologous substrates to the intestinal mucosa, as proposed previously for *Salmonella*-based vaccines (Rüssmann et al., 1998). Finally, immunomodulatory fragments of VopZ coupled to cell-permeable peptides could have therapeutic utility for patients with inflammatory conditions.

EXPERIMENTAL PROCEDURES

Bacterial Strains, Plasmids, and Culture Conditions

All strains are derived from RIMD2210633 (Makino et al., 2003). *vscN1*, *vscN2*, and *vscN1/vscN2* strains have been previously described by Hiyoshi et al. (2010). Additional mutants, including *vpa1343*, *vpa1350*, *vscN1 vopZ′* , and *vscN1 vopZΔ38–62* strains, were created by allele exchange using suicide vector pDM4 as previously described (Zhou et al., 2008). Plasmids pVopZ-His (for *vopZ* complementation), pVopZ-CyaA, pVopZΔ38–62-CyaA, pVopV-CyaA, and pVtrB were constructed using the vector pMMB207 (Morales et al., 1991) and introduced into *V. parahaemolyticus* strains via conjugation. HA-fusion constructs for full-length and truncated *vopZ* were constructed in pCMVHA (Clontech). Strains were cultured in LB medium at 37°C and supplemented with appropriate antibiotics. Expression vectors for FLAG-tagged human TAK1 and MKK6 have previously been described by Paquette et al. (2012). Recombinant $MKK6^{K82A}$ was purified as previously described by Paquette et al. (2012).

Eukaryotic Cell Lines and Culture Conditions

HeLa, Caco-2, and HEK293 cells were routinely maintained in DMEM (GIBCO) supplemented with 10% FBS (Clontech) at 37°C with 5% CO_2. For in vitro infection assays, bacterial cells were grown in LB supplemented with 0.04% sodium cholate for 2 hr to induce the expression of T3SS2.

2D Gel Analysis and Western Blot Analysis of Bacterial Proteins

To obtain proteins for 2D PAGE analysis, RIMD2210633 *vscN1* pVtrB and RIMD2210633 *vscN1 vscN2* pVtrB were cultured in DMEM containing 1 mM IPTG to induce expression of the T3SS2 activator, VtrB. After 3 hr of growth, cells were removed by centrifugation and filtration, and DIGE analysis was performed on the culture supernatant by Applied Biomics (Hayward, CA, USA). Western blot analysis was performed on cell pellets and supernatants from bacteria cultured in LB supplemented with 1 mM IPTG.

Effector-CyaA Fusion Protein-Based Analysis of Effector Translocation

Caco-2 cells were cultured for 10 days to achieve differentiation. Differentiated Caco-2 cells were infected with RIMD2210633 *vscN1* and RIMD2210633 *vscN1 vscN2* containing pCyaA, pVopZ-CyaA, pVopZΔ38–62-CyaA, or pVopV-CyaA for 1 hr in the presence of 0.04% sodium cholate and then cAMP levels were determined by ELISA as described previously (Zhou et al., 2012b).

Immunofluorescence Detection of VopV Translocation

HeLa cells grown overnight on glass coverslips were infected with *V. parahaemolyticus* overexpressing *vtrB* for 1 hr before being fixed with 4% formalin. Fixed cells were blocked with PBS containing 3% BSA for 1 hr, then VopV was detected with rabbit anti-VopV antisera (generously provided by Dr. Toshio Kodama) and FITC-goat anti-rabbit IgG (Sigma-Aldrich). Actin was stained with rhodamine phalloidin, and DNA was stained with DAPI.

Transfection and Visualization of VopZ within HeLa Cells

HeLa cells grown overnight on coverslips were transfected with HA-VopZ expression constructs using Lipofectamine 2000 (Life Technologies). Twenty-four hours after transfection, cells were fixed with 4% formalin, and full-length and truncated VopZs were detected by immunofluorescence using anti-HA (Sigma-Aldrich) and FITC-conjugated anti-mouse IgG (Sigma-Aldrich).

p65 Translocation Assays

HeLa cells grown overnight on coverslips were transfected with HA-VopZ expression constructs for 24 hr or infected with *V. parahaemolyticus* strains for 1 hr in the presence of 0.04% sodium cholate. After treatment with TNF-α (R&D Systems; 20 ng/ml) for 1 hr, cells were fixed, and p65 localization was detected using anti-p65 (Cell Signaling). For each of three transfection experiments, p65 localization was assessed in 30 cells with detectable VopZ. For each of three infection experiments, p65 localization was determined in 30 randomly selected cells. For in vivo assays of p65 translocation, frozen sections of distal small intestines from the rabbits infected with *V. parahaemolyticus* for 28 hr were stained with anti-p65 primary antibody (Cell Signaling) and Alexa Fluor 568 goat anti-mouse IgG secondary antibody. Nuclei were stained with DAPI. Localization of p65 was determined in three fields with 30 cells/field.

NF-κB Activity and IL-8 Production in HEK293 and HeLa Cells

HEK293 cells in which GFP reporter expression is controlled by four tandem NF-κB sites (Gewurz et al., 2012) were infected with *V. parahaemolyticus* for 90 min in the presence of 0.04% sodium cholate and then infection was terminated by addition of gentamicin (200 ng/ml). Cells were then cultured an additional 4–5 hr, either in the presence or absence of TNF-α (1 ng/ml). GFP expression was detected via FACS Calibur (BD; Gewurz et al., 2012). For assays of IL-8 production, HEK293 cells or HeLa cells were infected with *V. parahaemolyticus* for 90 min, then treated with TNF-α (2 ng/ml; HEK293) or IL-1β (R&D Systems, 25 ng/ml; HeLa) or left untreated for 90 min. IL-8 in culture supernatant was then measured via ELISA (BD).

Western Blot Analyses of Host Proteins

HEK293 cells were infected with *V. parahaemolyticus* at an approximate moi of 5:1 for 90 min in the presence of 0.04% sodium cholate, and infection was terminated by addition of gentamicin (200 ng/ml). Infected cells were stimulated with TNF-α (1 ng/ml), then lysed as described (Gewurz et al., 2011) at the indicated time points poststimulation. Protein samples were electrophoresed on SDS-PAGE 10% gels, transferred to nitrocellulose membranes, and probed with Cell Signaling antibodies against IκBα (#9242), phospho-JNK (#9251), phospho-p38 (#9211), total JNK(#9252), and total p38(#9212). For detection of endogenous (but not transfected) phospho-TAK1, cells were stimulated with TNF-α in the presence of 50 nM Calyculin A, and pTAK1 was detected with #4536. Also used were anti-Tubulin (Sigma-Aldrich; T5168) and anti-LMP1 monoclonal S12.

Epistasis Experiments—HEK293 cells (4×10^5) were reverse transfected in 6-well plates with FLAG-TAK1 or MKK6 using Effectene (QIAGEN), as indicated. Forty-eight hours later, cells were split 1:2 into 12-well plates and then infected 24 hr later with the indicated bacterial strains for 90 min. Whole-cell lysates were subjected to SDS-PAGE and western blot as described above. Of note, cells were not treated with Calyculin A for pTAK1 detection.

Kinase Assay—HEK293 cells (3×10^6) were Effectene reverse transfected with FLAG-TAK1 or FLAG-TAK1-K63W (a kinase-dead mutant). Forty-eight hours later, cells were split 1:2 and then 24 hr thereafter, infected for 90 min with the indicated bacterial strain. FLAG-TAK1 was then immunoprecipitated and used in cold in vitro kinase reactions with recombinant HIS-tagged MKK6-K82A, as previously described by Paquette et al. (2012). Kinase assays were subject to SDS-PAGE, and western blots were probed for pTAK1 and pMKK6, and reprobed with anti-FLAG (Sigma-Aldrich M2 antibody) for total TAK1.

Detection of Noncanonical NF-κB Activation

HEK293 cells were infected with *V. parahaemolyticus* for 90 min, and infection was terminated by gentamicin addition (200 ng/ml). Infected cells were subsequently stimulated with LMP1 residue 1–231 expression for approximately 8 hr, lysed with 1% NP40 lysis buffer, and electrophoresed as described above. Membranes were probed with anti-p100/p52 (Millipore; #05-361).

Infection of Infant Rabbits

Infant rabbits were infected as described previously (Ritchie et al., 2012). Briefly, cimetidine-treated rabbits were orogastrically inoculated with 10^9 cfu of *V. parahaemolyticus*, and bacterial colonization (cfu/g intestinal tissue) and fluid accumulation were measured 38 hr postinfection. Translocation of p65 and actin localization were determined 28 hr postinfection in order to assess less-disrupted tissues. Fluid accumulation ratios for the distal small intestine were determined by isolating an approximately 5 cm length of tissue using silk ligatures. The intestinal section was weighed and then cut every 0.5 cm to release any luminal fluid, and the tissue pieces were reweighed. The fluid accumulation ratio was calculated as the weight of fluid divided by the weight of the drained tissue. Histological scores were graded by a pathologist.

All animal experiments were performed in accordance with a protocol approved by the Harvard IACUC.

Supplementary Material

Refer to Web version on PubMed Central for supplementary material.

Acknowledgments

We thank Dr. Carlos Blondel for pointing out to us the structural similarity of VPA1343 and PrgI, Dr. Toshio Kodoma for antisera and *vscN1* and *vscN1 vscN2 V. parahaemolyticus* strains, Dr. Rod Bronson for scoring infant rabbit histopathology, Drs. Neal Silverman and Kate Fitzgerald for human FLAG-TAK1, FLAG-MKK6, and HIS-MKK6K82A vectors, and Jennifer Oghene for assistance with the infant rabbit studies. Grants from HHMI and NIH-AI-R37 42347 to M.K.W., NERCE Fellowship (U54 AI 057159) to X.Z., and NIH K08 CA140780 and Burroughs Wellcome Medical Scientist Career award to B.E.G., and RO1 CA085180 to E.K. supported this work.

References

Akeda Y, Kodama T, Saito K, Iida T, Oishi K, Honda T. Identification of the *Vibrio parahaemolyticus* type III secretion system 2-associated chaperone VocC for the T3SS2-specific effector VopC. FEMS Microbiol Lett. 2011; 324:156–164. [PubMed: 22092817]

Baldwin AS. Regulation of cell death and autophagy by IKK and NF-κB: critical mechanisms in immune function and cancer. Immunol Rev. 2012; 246:327–345. [PubMed: 22435564]

Bhattacharjee RN, Park KS, Kumagai Y, Okada K, Yamamoto M, Uematsu S, Matsui K, Kumar H, Kawai T, Iida T, et al. VP1686, a *Vibrio* type III secretion protein, induces toll-like receptor-independent apoptosis in macrophage through NF-kappaB inhibition. J Biol Chem. 2006; 281:36897–36904. [PubMed: 16984916]

Broberg CA, Calder TJ, Orth K. *Vibrio parahaemolyticus* cell biology and pathogenicity determinants. Microbes Infect. 2011; 13:992–1001. [PubMed: 21782964]

Burdette DL, Yarbrough ML, Orvedahl A, Gilpin CJ, Orth K. *Vibrio parahaemolyticus* orchestrates a multifaceted host cell infection by induction of autophagy, cell rounding, and then cell lysis. Proc Natl Acad Sci USA. 2008; 105:12497–12502. [PubMed: 18713860]

Burdette DL, Yarbrough ML, Orth K. Not without cause: *Vibrio parahaemolyticus* induces acute autophagy and cell death. Autophagy. 2009; 5:100–102. [PubMed: 19011375]

Coburn B, Sekirov I, Finlay BB. Type III secretion systems and disease. Clin Microbiol Rev. 2007; 20:535–549. [PubMed: 17934073]

Cornelis GR. The type III secretion injectisome. Nat Rev Microbiol. 2006; 4:811–825. [PubMed: 17041629]

Dai L, Aye Thu C, Liu XY, Xi J, Cheung PC. TAK1, more than just innate immunity. IUBMB Life. 2012; 64:825–834. [PubMed: 22941947]

Dean P. Functional domains and motifs of bacterial type III effector proteins and their roles in infection. FEMS Microbiol Rev. 2011; 35:1100–1125. [PubMed: 21517912]

DeVinney R, Stein M, Reinscheid D, Abe A, Ruschkowski S, Finlay BB. Enterohemorrhagic *Escherichia coli* O157:H7 produces Tir, which is translocated to the host cell membrane but is not tyrosine phosphorylated. Infect Immun. 1999; 67:2389–2398. [PubMed: 10225900]

Galán JE. Common themes in the design and function of bacterial effectors. Cell Host Microbe. 2009; 5:571–579. [PubMed: 19527884]

Gewurz BE, Mar JC, Padi M, Zhao B, Shinners NP, Takasaki K, Bedoya E, Zou JY, Cahir-McFarland E, Quackenbush J, Kieff E. Canonical NF-kappaB activation is essential for Epstein-Barr virus latent membrane protein 1 TES2/CTAR2 gene regulation. J Virol. 2011; 85:6764–6773. [PubMed: 21543491]

Gewurz BE, Towfic F, Mar JC, Shinners NP, Takasaki K, Zhao B, Cahir-McFarland ED, Quackenbush J, Xavier RJ, Kieff E. Genome-wide siRNA screen for mediators of NF-κB activation. Proc Natl Acad Sci USA. 2012; 109:2467–2472. [PubMed: 22308454]

Hayden MS, Ghosh S. NF-κB in immunobiology. Cell Res. 2011; 21:223–244. [PubMed: 21243012]

Hayden MS, Ghosh S. NF-κB, the first quarter-century: remarkable progress and outstanding questions. Genes Dev. 2012; 26:203–234. [PubMed: 22302935]

Hiyoshi H, Kodama T, Iida T, Honda T. Contribution of *Vibrio parahaemolyticus* virulence factors to cytotoxicity, enterotoxicity, and lethality in mice. Infect Immun. 2010; 78:1772–1780. [PubMed: 20086084]

Hiyoshi H, Kodama T, Saito K, Gotoh K, Matsuda S, Akeda Y, Honda T, Iida T. VopV, an F-actin-binding type III secretion effector, is required for *Vibrio parahaemolyticus*-induced enterotoxicity. Cell Host Microbe. 2011; 10:401–409. [PubMed: 22018240]

Hoffmann E, Dittrich-Breiholz O, Holtmann H, Kracht M. Multiple control of interleukin-8 gene expression. J Leukoc Biol. 2002; 72:847–855. [PubMed: 12429706]

Kajino T, Ren H, Iemura SI, Natsume T, Stefansson B, Brautigan DL, Matsumoto K, Ninomiya-Tsuji J. Protein phosphatase 6 down-regulates TAK1 kinase activation in the IL-1 signaling pathway. J Biol Chem. 2006; 281:39891–39896. [PubMed: 17079228]

Kajino-Sakamoto R, Inagaki M, Lippert E, Akira S, Robine S, Matsumoto K, Jobin C, Ninomiya-Tsuji J. Enterocyte-derived TAK1 signaling prevents epithelium apoptosis and the development of ileitis and colitis. J Immunol. 2008; 181:1143–1152. [PubMed: 18606667]

Kajino-Sakamoto R, Omori E, Nighot PK, Blikslager AT, Matsumoto K, Ninomiya-Tsuji J. TGF-beta-activated kinase 1 signaling maintains intestinal integrity by preventing accumulation of reactive oxygen species in the intestinal epithelium. J Immunol. 2010; 185:4729–4737. [PubMed: 20855879]

Kelley LA, Sternberg MJE. Protein structure prediction on the Web: a case study using the Phyre server. Nat Protoc. 2009; 4:363–371. [PubMed: 19247286]

Kishimoto K, Matsumoto K, Ninomiya-Tsuji J. TAK1 mitogen-activated protein kinase kinase kinase is activated by autophosphorylation within its activation loop. J Biol Chem. 2000; 275:7359–7364. [PubMed: 10702308]

Kodama T, Rokuda M, Park KS, Cantarelli VV, Matsuda S, Iida T, Honda T. Identification and characterization of VopT, a novel ADP-ribosyltransferase effector protein secreted via the *Vibrio parahaemolyticus* type III secretion system 2. Cell Microbiol. 2007; 9:2598–2609. [PubMed: 17645751]

Kodama T, Hiyoshi H, Gotoh K, Akeda Y, Matsuda S, Park KS, Cantarelli VV, Iida T, Honda T. Identification of two translocon proteins of *Vibrio parahaemolyticus* type III secretion system 2. Infect Immun. 2008; 76:4282–4289. [PubMed: 18541652]

Liverman ADB, Cheng HC, Trosky JE, Leung DW, Yarbrough ML, Burdette DL, Rosen MK, Orth K. Arp2/3-independent assembly of actin by *Vibrio* type III effector VopL. Proc Natl Acad Sci USA. 2007; 104:17117–17122. [PubMed: 17942696]

Luftig M, Yasui T, Soni V, Kang MS, Jacobson N, Cahir-McFarland E, Seed B, Kieff E. Epstein-Barr virus latent infection membrane protein 1 TRAF-binding site induces NIK/IKK alpha-dependent noncanonical NF-kappaB activation. Proc Natl Acad Sci USA. 2004; 101:141–146. [PubMed: 14691250]

Makino K, Oshima K, Kurokawa K, Yokoyama K, Uda T, Tagomori K, Iijima Y, Najima M, Nakano M, Yamashita A, et al. Genome sequence of *Vibrio parahaemolyticus*: a pathogenic mechanism distinct from that of *V cholerae*. Lancet. 2003; 361:743–749. [PubMed: 12620739]

Matlawska-Wasowska K, Finn R, Mustel A, O'Byrne CP, Baird AW, Coffey ET, Boyd A. The *Vibrio parahaemolyticus* Type III Secretion Systems manipulate host cell MAPK for critical steps in pathogenesis. BMC Microbiol. 2010; 10:329. [PubMed: 21192810]

Meinzer U, Barreau F, Esmiol-Welterlin S, Jung C, Villard C, Léger T, Ben-Mkaddem S, Berrebi D, Dussaillant M, Alnabhani Z, et al. *Yersinia pseudotuberculosis* effector YopJ subverts the Nod2/RICK/TAK1 pathway and activates caspase-1 to induce intestinal barrier dysfunction. Cell Host Microbe. 2012; 11:337–351. [PubMed: 22520462]

Mittal R, Peak-Chew SY, McMahon HT. Acetylation of MEK2 and I kappa B kinase (IKK) activation loop residues by YopJ inhibits signaling. Proc Natl Acad Sci USA. 2006; 103:18574–18579. [PubMed: 17116858]

Morales VM, Bäckman A, Bagdasarian M. A series of wide-host-range low-copy-number vectors that allow direct screening for recombinants. Gene. 1991; 97:39–47. [PubMed: 1847347]

Mukherjee S, Keitany G, Li Y, Wang Y, Ball HL, Goldsmith EJ, Orth K. *Yersinia* YopJ acetylates and inhibits kinase activation by blocking phosphorylation. Science. 2006; 312:1211–1214. [PubMed: 16728640]

Nenci A, Becker C, Wullaert A, Gareus R, van Loo G, Danese S, Huth M, Nikolaev A, Neufert C, Madison B, et al. Epithelial NEMO links innate immunity to chronic intestinal inflammation. Nature. 2007; 446:557–561. [PubMed: 17361131]

Omori E, Inagaki M, Mishina Y, Matsumoto K, Ninomiya-Tsuji J. Epithelial transforming growth factor β-activated kinase 1 (TAK1) is activated through two independent mechanisms and regulates reactive oxygen species. Proc Natl Acad Sci USA. 2012; 109:3365–3370. [PubMed: 22331902]

Paquette N, Conlon J, Sweet C, Rus F, Wilson L, Pereira A, Rosadini CV, Goutagny N, Weber AN, Lane WS, et al. Serine/threonine acetylation of TGFβ-activated kinase (TAK1) by *Yersinia pestis*

YopJ inhibits innate immune signaling. Proc Natl Acad Sci USA. 2012; 109:12710–12715. [PubMed: 22802624]

Park KS, Ono T, Rokuda M, Jang MH, Okada K, Iida T, Honda T. Functional characterization of two type III secretion systems of *Vibrio parahaemolyticus*. Infect Immun. 2004; 72:6659–6665. [PubMed: 15501799]

Piñeyro P, Zhou X, Orfe LH, Friel PJ, Lahmers K, Call DR. Development of two animal models to study the function of *Vibrio parahaemolyticus* type III secretion systems. Infect Immun. 2010; 78:4551–4559. [PubMed: 20823199]

Qadri F, Alam MS, Nishibuchi M, Rahman T, Alam NH, Chisti J, Kondo S, Sugiyama J, Bhuiyan NA, Mathan MM, et al. Adaptive and inflammatory immune responses in patients infected with strains of *Vibrio parahaemolyticus*. J Infect Dis. 2003; 187:1085–1096. [PubMed: 12660923]

Ritchie JM, Rui H, Zhou X, Iida T, Kodoma T, Ito S, Davis BM, Bronson RT, Waldor MK. Inflammation and disintegration of intestinal villi in an experimental model for *Vibrio parahaemolyticus*-induced diarrhea. PLoS Pathog. 2012; 8:e1002593. [PubMed: 22438811]

Rüssmann H, Shams H, Poblete F, Fu Y, Galán JE, Donis RO. Delivery of epitopes by the *Salmonella* type III secretion system for vaccine development. Science. 1998; 281:565–568. [PubMed: 9677200]

Sakurai H. Targeting of TAK1 in inflammatory disorders and cancer. Trends Pharmacol Sci. 2012; 33:522–530. [PubMed: 22795313]

Shimohata T, Takahashi A. Diarrhea induced by infection of *Vibrio parahaemolyticus*. J Med Invest. 2010; 57:179–182. [PubMed: 20847516]

Su YC, Liu C. *Vibrio parahaemolyticus*: a concern of seafood safety. Food Microbiol. 2007; 24:549–558. [PubMed: 17418305]

Sun SC. non-canonical NF-κB signaling pathway. Cell Res. 2011; 21:71–85. [PubMed: 21173796]

Trosky JE, Li Y, Mukherjee S, Keitany G, Ball H, Orth K. VopA inhibits ATP binding by acetylating the catalytic loop of MAPK kinases. J Biol Chem. 2007; 282:34299–34305. [PubMed: 17881352]

Zhang L, Ding X, Cui J, Xu H, Chen J, Gong YN, Hu L, Zhou Y, Ge J, Lu Q, et al. Cysteine methylation disrupts ubiquitin-chain sensing in NF-κB activation. Nature. 2012; 481:204–208. [PubMed: 22158122]

Zhou X, Shah DH, Konkel ME, Call DR. Type III secretion system 1 genes in *Vibrio parahaemolyticus* are positively regulated by ExsA and negatively regulated by ExsD. Mol Microbiol. 2008; 69:747–764. [PubMed: 18554322]

Zhou X, Konkel ME, Call DR. Vp1659 is a *Vibrio parahaemolyticus* type III secretion system 1 protein that contributes to translocation of effector proteins needed to induce cytolysis, autophagy, and disruption of actin structure in HeLa cells. J Bacteriol. 2010; 192:3491–3502. [PubMed: 20418402]

Zhou X, Nydam SD, Christensen JE, Konkel ME, Orfe L, Friel P, Call DR. Identification of potential type III secretion proteins via heterologous expression of *Vibrio parahaemolyticus* DNA. Appl Environ Microbiol. 2012a; 78:3492–3494. [PubMed: 22389365]

Zhou X, Ritchie JM, Hiyoshi H, Iida T, Davis BM, Waldor MK, Kodama T. The hydrophilic translocator for *Vibrio parahaemolyticus*, T3SS2, is also translocated. Infect Immun. 2012b; 80:2940–2947. [PubMed: 22585964]

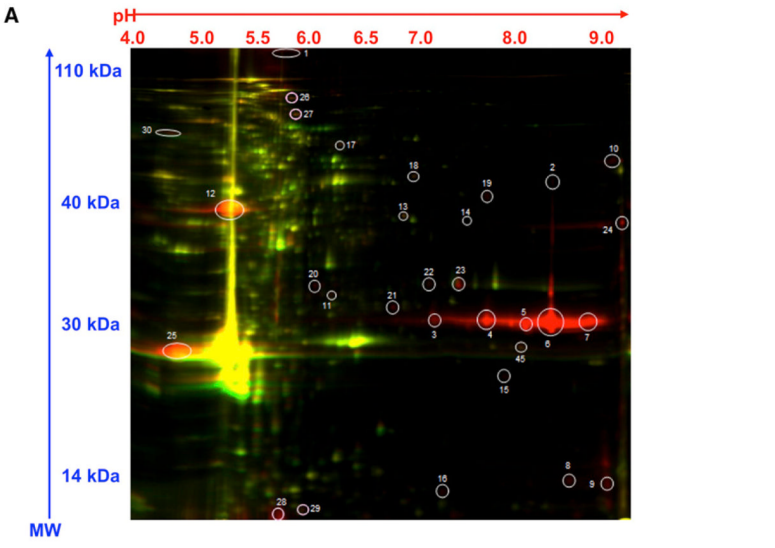

C

Spot	Name (locus)	Putative function/motif (ref)	T3SS2
1	VopV (Vpa1357)	effector, binds actin (Hiyoshi et al., 2011)	Y
2-9	VopD2 (Vpa1361)	translocator (Kodama et al., 2008)	Y
10,11	VopL (Vpa1370)	effector, actin nucleator (Liverman et al., 2007)	Y
12	VopW (Vpa1345)	translocator (Zhou et al, 2012)	Y
13-19	non-vibrio proteins		ND
20	VopZ (Vpa1336)	effector (this paper)	Y*
21	VopT (Vpa1327)	effector, ADP-ribosyltransferase (Kodama et al., 2007)	Y
22	VopA (Vpa1346)	effector, Ser/Thr acetyltransferase (Trosky et al., 2007)	Y
23	Imp (Vp0323)	Immunogenic protein	N
24	VopC (Vpa1321)	effector, deamidase (Akeda et al., 2011)	Y
25	(Vpa 1350)	DUF812, possible T3SS2 component (this paper)	Y*
26	ClpB (Vp0561)	?protease, AAA ATPase (Makino et al., 2003)	ND
27	PflD(Vp0994)	Pyruvate formate lyase (Makino et al., 2003)	ND
28	(Vpa1343)	possible needle protein (this paper)	ND
29	VopcC (Vpa1334)	chaperone for VopC (Akeda et al., 2011)	ND
30	GlyA(Vp0715)	serine hydroxymethyltransferase	ND

Figure 1. Identification of T3SS2-Secreted Polypeptides

(A) DIGE of supernatant-derived proteins from a T3SS1-deficient strain (RIMD2210633 *vscN1*; red) and a T3SS1/T3SS2-deficient strain (RIMD2210633 *vscN1 vscN2*; green). Spots selected for MALDI tandem mass spectrometry are circled, and protein identities and functions are indicated below.

(B) Schematic depiction of the T3SS2 region from *V. parahaemolyticus* RIMD2210633, including most genes from *vpa1321* to *vpa1370*. Genes encoding effectors are colored red; genes encoding structural components are colored gray. The transcriptional regulator *vtrB* (*vpa1348)* is colored black.

(C) Identity of the spots identified from DIGE and mass spectrometry. Black print shows proteins encoded in T3SS2, gray print indicates proteins encoded outside of T3SS2, and red type indicates effector proteins. Final column shows whether T3SS2-dependent secretion has been confirmed: yes (Y), no (N), not determined (ND). Asterisk indicates previously unidentified T3SS2-secreted proteins.

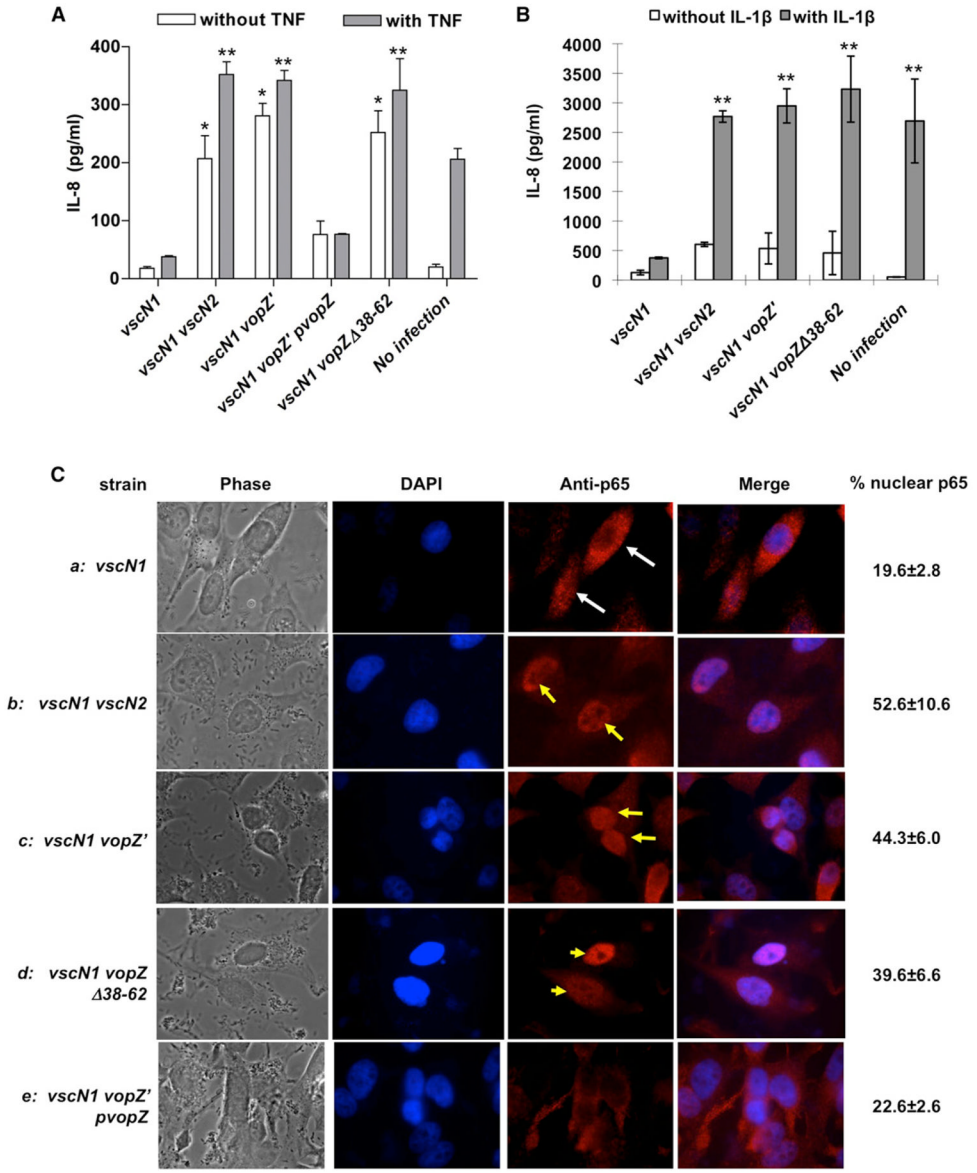

Figure 2. VopZ Inhibits Release of IL-8 and Nuclear Translocation of p65

(A) IL-8 release by HEK293 cells was monitored following infection with the indicated strains of *V. parahaemolyticus* using cells either treated (gray bars) or not treated (white bars) with TNF-α.

(B) IL-8 release by HeLa cells was monitored following infection with the indicated strains of *V. parahaemolyticus* using cells either treated (gray bars) or not treated (white bars) with IL-1β.

(C) p65 was visualized using immunofluorescence microscopy in HeLa cells that were infected (1 hr) with the indicated strains of *V. parahaemolyticus*, then treated with TNF-α (20 ng/ml). Nuclei were visualized with DAPI (blue), and p65 was detected with p65 antisera (red). White arrows indicate cells with cytoplasmic p65; yellow arrows mark cells with nuclear p65. Mean values (n = 3) and SD are shown.

For (A) and (B), IL-8 levels in supernatants were measured via ELISA; mean values (n = 2) and SD are shown. The asterisk (*) indicates statistical difference ($p < 0.05$) when compared to *vscN1*-infected cells without TNF treatment; the double asterisks (**) indicate statistical

difference ($p < 0.05$) when compared to *vscN1*-infected cells with TNF-α or IL-1β treatment. See also Figure S4.

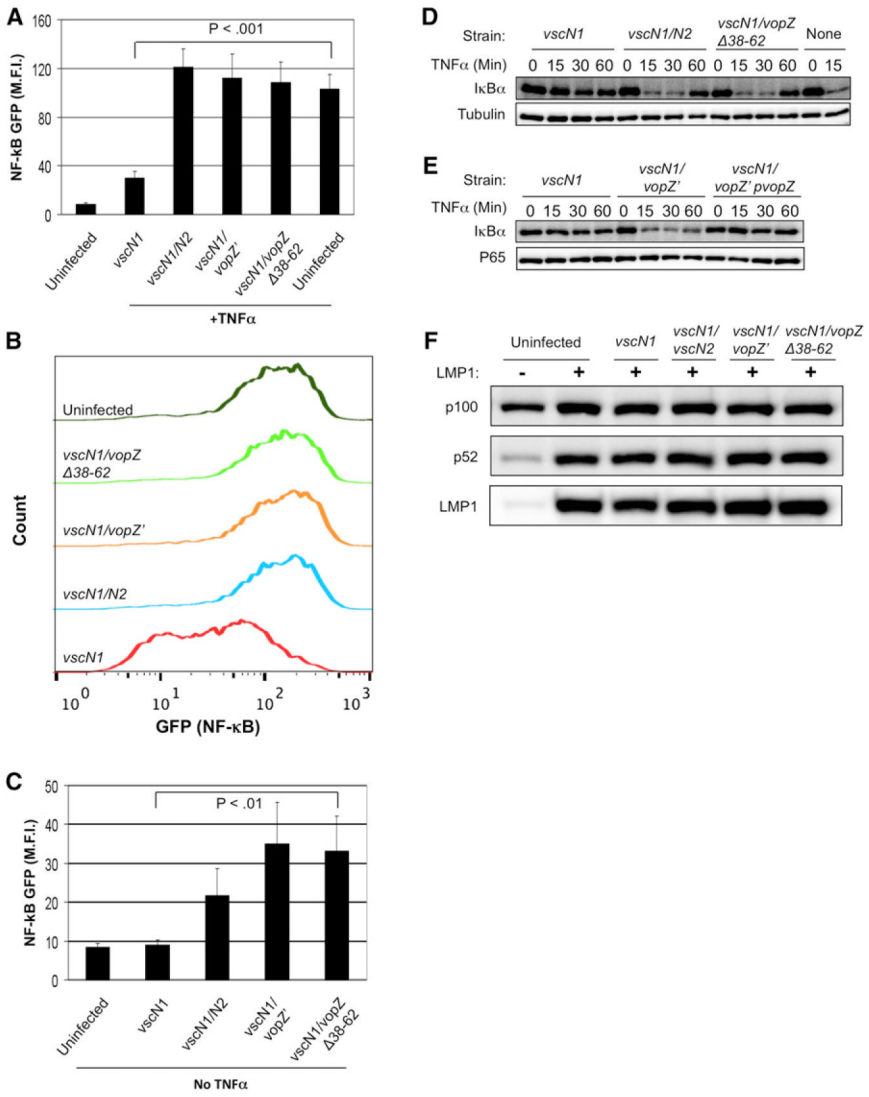

Figure 3. VopZ Inhibits Canonical NF-κB Pathway Activation

(A and B) HEK293 NF-κB GFP reporter cells were infected for 90 min and then stimulated by TNF-α (1 ng/ml) for 6 hr. GFP mean fluorescence intensity (M.F.I.) (A) and representative FACS overlay plots

(B) are shown.

(C) HEK293 NF-κB GFP reporter cells were infected for 90 min, and NF-κB activity was analyzed 15 hr later.

(D and E) VopZ inhibits IκBα turnover. HEK293 cells were infected with *V. parahaemolyticus* strains for 90 min, then stimulated by TNF-α (1 ng/ml) for the indicated times. Tubulin (D) and p65 (E) are loading controls.

(F) HEK293 cells were infected with the indicated strains for 90 min and then noncanonical NF-κB signaling was stimulated by LMP1 expression for 12 hr. Noncanonical NF-κB pathway activation induces cleavage of p100 into p52.

For (A) and (C), duplicate samples from three independent experiments were used to obtain M.F.I. and SD data. Student's two-tailed paired t test p values are denoted. All samples bracketed were found to differ significantly from the *vscN1* control strain. Western blots representative of three independent experiments are shown (D–F).

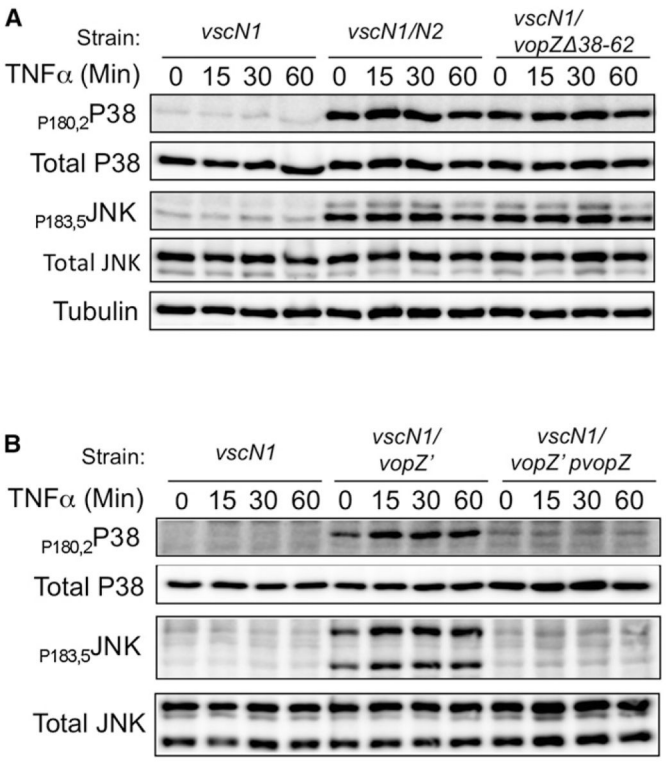

Figure 4. VopZ Inhibits MAPK Pathway Activation

(A and B) Activation of p38 and JNK was assessed using antibodies to total and phosphorylated forms of proteins. HEK293 cells were infected with *V. parahaemolyticus* strains for 90 min and then stimulated by TNF-α (1 ng/ml). Western blots representative of three independent experiments are shown.

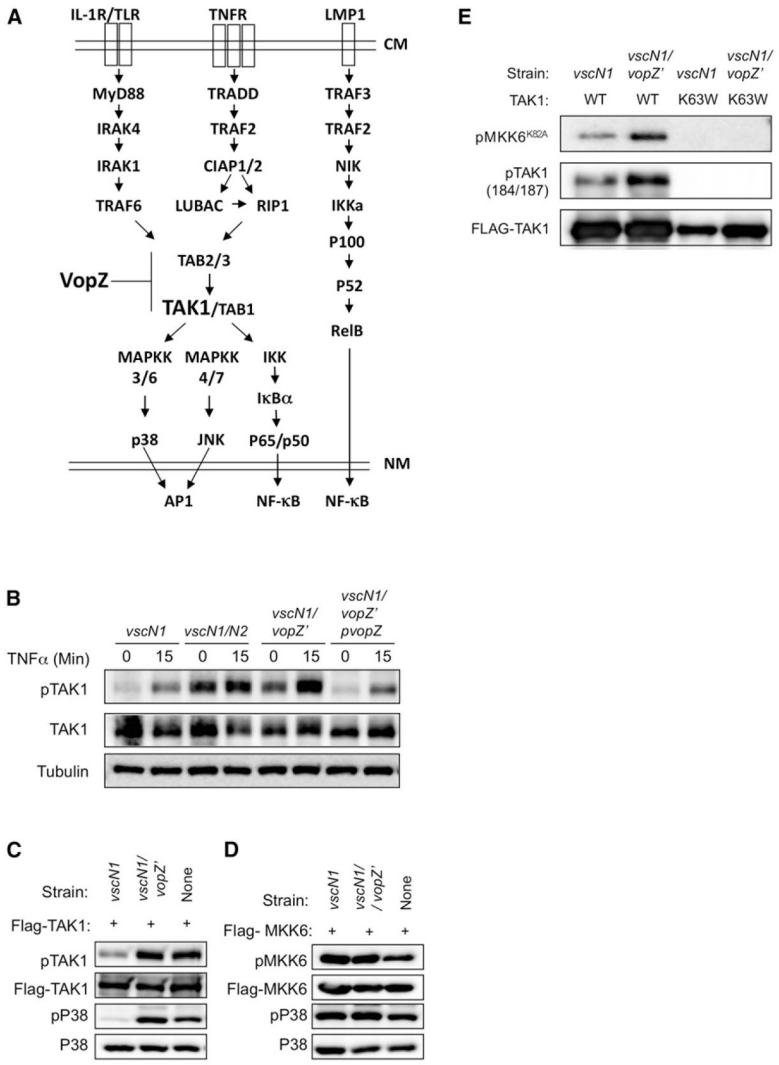

Figure 5. VopZ Inhibits TAK1 Activation

(A) Schematic of signaling pathways leading to activation of MAPKs and canonical and noncanonical NF-κB, and possible site of VopZ action. CM, cell membrane; NM, nuclear membrane.

(B) HEK293 cells were infected with *V. parahaemolyticus* strains for 90 min and then stimulated by TNF-α (1 ng/ml). Activation of TAK1 was assessed using antibodies to total and T184/T187-phosphorylated TAK1.

(C and D) TAK1, but not MKK6, autophosphorylation and activity are inhibited by VopZ. FLAG-TAK1 or MKK6 was transiently expressed in HEK293 cells, which were then infected for 90 min with the indicated strains. Activation of TAK1, MKK6, and P38 was assessed using antibodies to total and phosphorylated forms of proteins.

(E) WT or K63W (kinase-deficient) TAK1 was immunopurified from transfected HEK293 cells that had been infected with the indicated strains for 90 min prior to harvest. TAK1 activity was monitored using a cold kinase assay, followed by detection of phosphorylated substrate (recombinant kinase-deficient MKK6-K82A) via immunoblotting. Phospho-and total TAK1 levels were also monitored by immunoblot. Western blots representative of three independent experiments are shown.

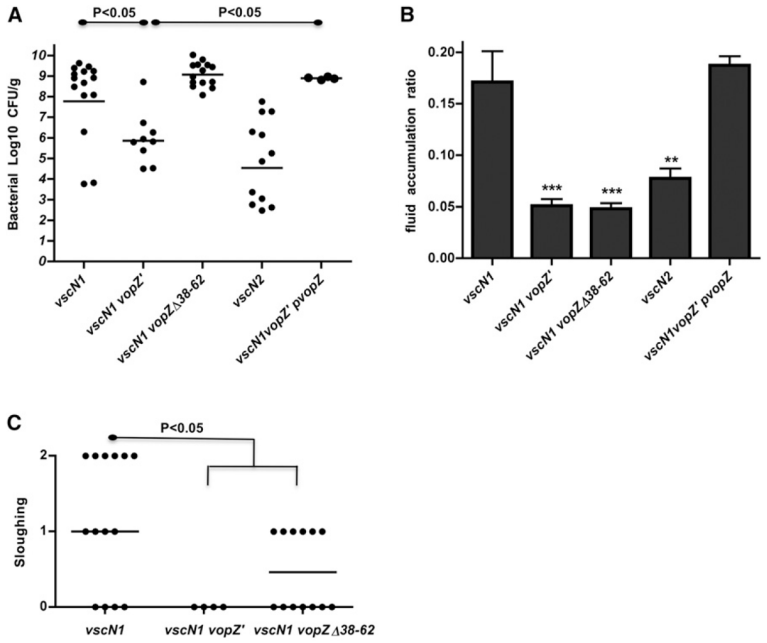

Figure 6. VopZ Makes Distinct and Genetically Separable Contributions to *V. parahaemolyticus* Colonization and Pathogenesis within the Infant Rabbit Small Intestine

Bacterial colonization (cfu/g) in intestinal tissue (A) and intestinal fluid accumulation ratios (B) for infant rabbits infected with the indicated strains of *V. parahaemolyticus* at ~38 hr postinfection. Lines in (A) show geometric means. Means and SEM, based on at least nine rabbits, are shown in (B). Data for the *vscN1* and *vscN2* strains were previously published (Ritchie et al., 2012). Tissue sloughing (C) in tissue from distal intestines of infected infant rabbits was scored as described (Ritchie et al., 2012); median values are indicated. Statistical significance was assessed with one-way ANOVA and Bonferroni's posttests: *$p < 0.05$, **$p < 0.01$, ***$p < 0.001$, or as indicated on the graphs.

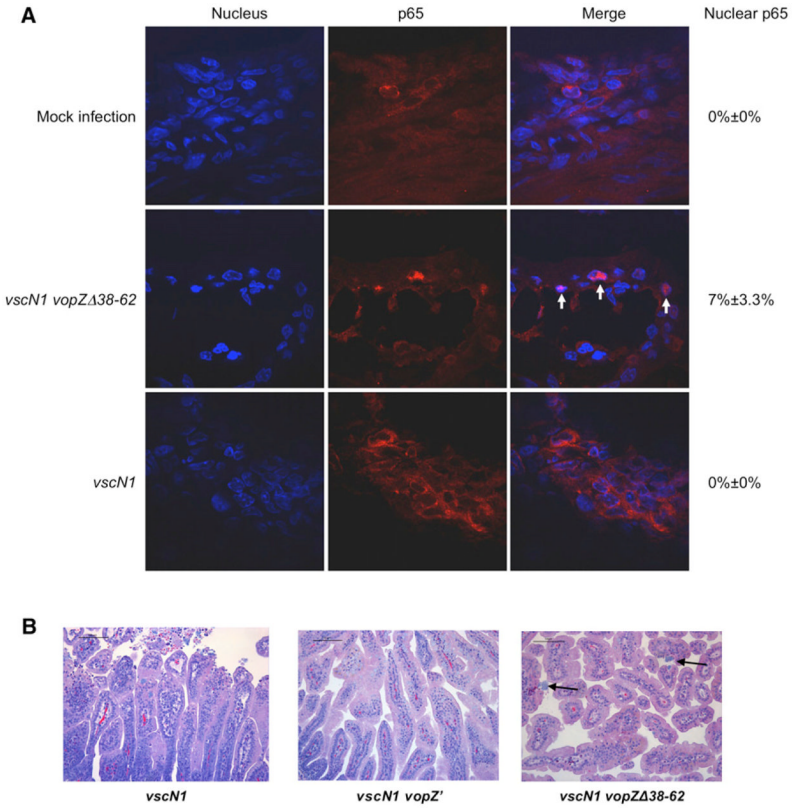

Figure 7. Production of VopZΔ38–62 In Vivo Is Associated with Increased Nuclear p65 and Reduced Disruption of the Intestinal Epithelium

(A) Immunofluorescence microscopy was used to detect p65 (red) in frozen sections of distal small intestines from rabbits infected with *V. parahaemolyticus* for 28 hr. Nuclei were stained with DAPI (blue). Arrows indicate nuclear p65.

(B) Tissue from the distal small intestines of rabbits infected with the indicated strains of *V. parahaemolyticus* for 38 hr was stained with H&E. Arrows indicate bacterial microcolonies.